

Lactea: Web-Based Spectrum-Preserving Multi-Resolution Visualization of the GAIA Star Catalog

SUPPLEMENTARY MATERIAL

Reem Alghamdi¹, Markus Hadwiger¹, Guido Reina², and Alberto Jaspe-Villanueva¹

¹King Abdullah University of Science and Technology (KAUST), Saudi Arabia

²Visualization Research Center (VISUS), University of Stuttgart, Germany

A Traversal cut-off strategies

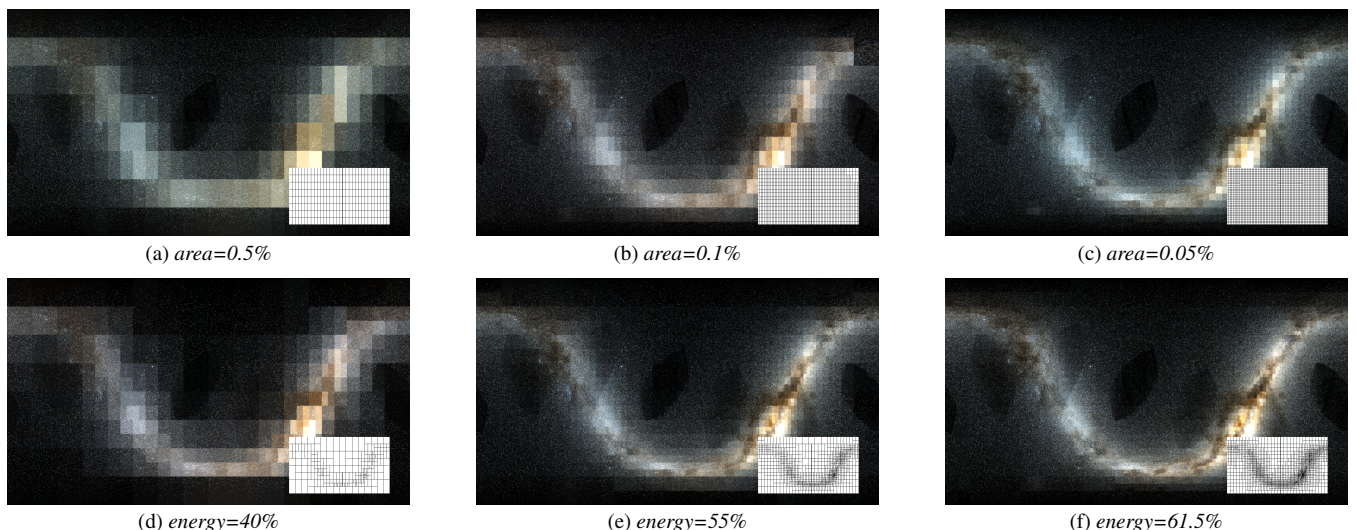


Figure 1: The first row shows the result using the area-based cutoff, while the second uses the energy-based cutoff. Images on the same column have similar numbers of patches and stars drawn to show that an energy-based cut-off is visually better with the same rendering budget. (a) draws the stars of 255 nodes and the patches of 256 nodes. Similarly, (d) draws the stars of 247 nodes and the patches of 248 nodes. (b) draws the stars of 1023 nodes and the patches of 1024 nodes, while (e) draws the stars of 1087 nodes and the patches of 1088 nodes. Lastly, (c) draws the stars of 2047 nodes and the patches of 2048 nodes, and (f) draws the stars of 2038 nodes and the patches of 2039 nodes.

We compare two cut-off strategies to control how the tree is traversed and where it is cut off.

Area-based cut-off. The tree is traversed until a node's projected area on the screen is smaller than a certain percentage of the total image. Once nodes are small enough, the branch is not traversed further, and the nodes at the graph cut are rendered as patches on the screen.

Energy-based cut-off. Nodes with higher total energy (the total of the node's energy with the energy of its subtree) and prioritized first by using a priority queue. Traversal continues by expanding the brightest nodes first. The traversal stops when the total energy of the loaded stars exceeds a user-defined percentage of the total energy of the shallowest nodes that fully fit within the view boundaries. For example, while viewing the whole dataset, the shallowest node that fits the view boundary is the root node, so the traversal will continue until the total energy is less than a percentage of the whole tree energy. Then, the remaining nodes are rendered as patches on the screen.

Multiresolution is usually based on the area. However, it is more useful to visit brighter nodes first in our algorithm. This way, brighter branches are prioritized over shallower, dimmer nodes, even if the latter occupy a more extensive area spatially. Figure 1 compares the classical area cut-off with the energy-based cut-off using an equirectangular projection of the whole dataset. The color is based on the photometric values. Energy-based cut-off results in an image with better details compared to the area-based cut-off, even when a very similar number of stars and patches are drawn.

B Progressive Rendering over Time

Figure 2 illustrates the progressive nature of the algorithm: the image improves as more stars are drawn. The region of interest can reach 80% of its final energy after loading a fraction of the data due to the algorithm's characteristic (i.e., shallower nodes contain brighter stars).

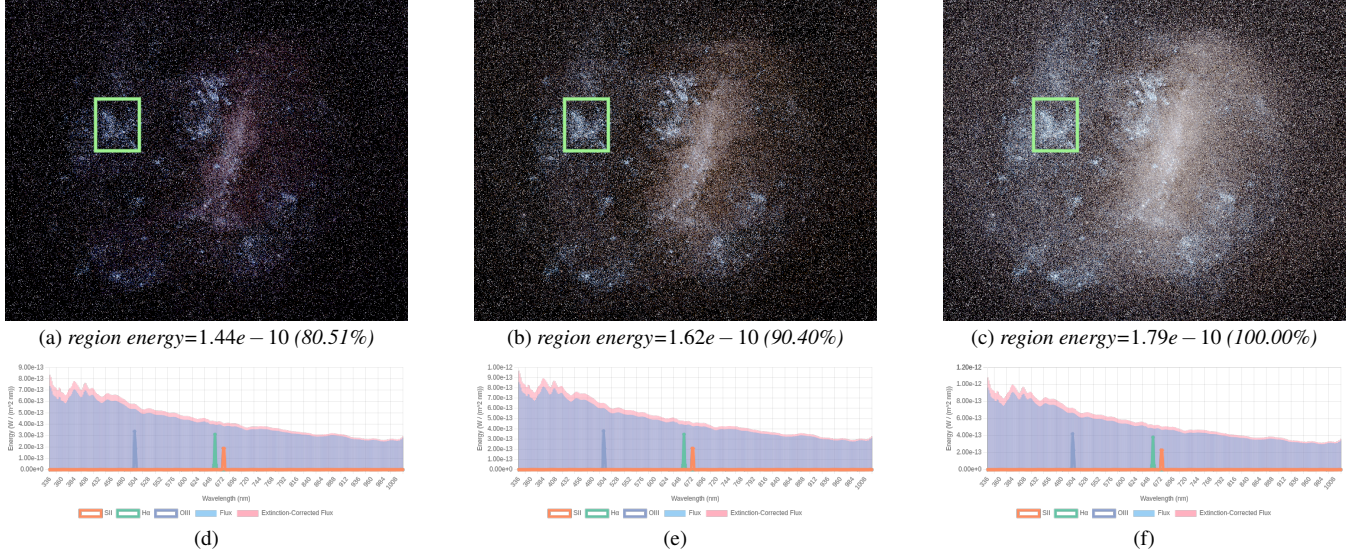


Figure 2: The first row shows the progressive rendering of the Large Magellanic Clouds. The second row is the selected region's spectrum over time. (a) the rendering after 28 seconds, drawing 4,740 stars. (b) the rendering after 58 seconds, drawing 10,524 stars. (c) the rendering after 156 seconds, drawing 23,915 stars.

C The User Interface

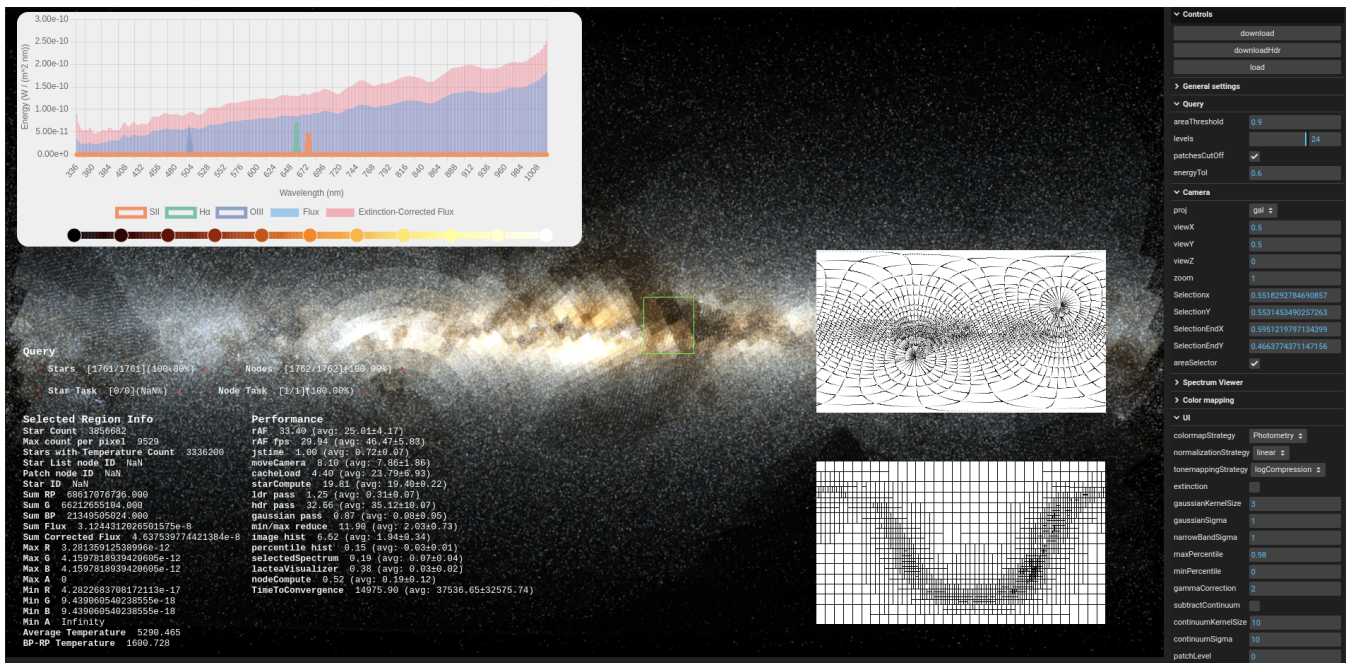


Figure 3: The user interface of Lactea's WebGPU implementation.

Our algorithm *Lactea* is implemented as an open-source, web-based tool to demonstrate the potential of spectral rendering and exploration. Figure 3 shows the user interface and the different rendering parameters controlling the resulting image. Rendering and spectral information are displayed to the user to show the overall performance, as well as the selected region's spectral data. The settings menu contains the camera configurations, cut-off strategy, and visualization-related settings such as tone mapping, spectral information to visualize, or use cases. The view bound and the traversed part of the tree are shown on the bottom right. The projected node boundaries are drawn on the right. The UI can be expanded to fill a scrolling page, and any UI element (e.g., the performance) can be hidden.

D Extended results

This section contains the full-resolution and extended images of the results presented in the paper. The extended version of Figure 10 in the paper is shown in Figure 4. Similarly, the extended version of Figure 11 in the paper is in Figure 5.

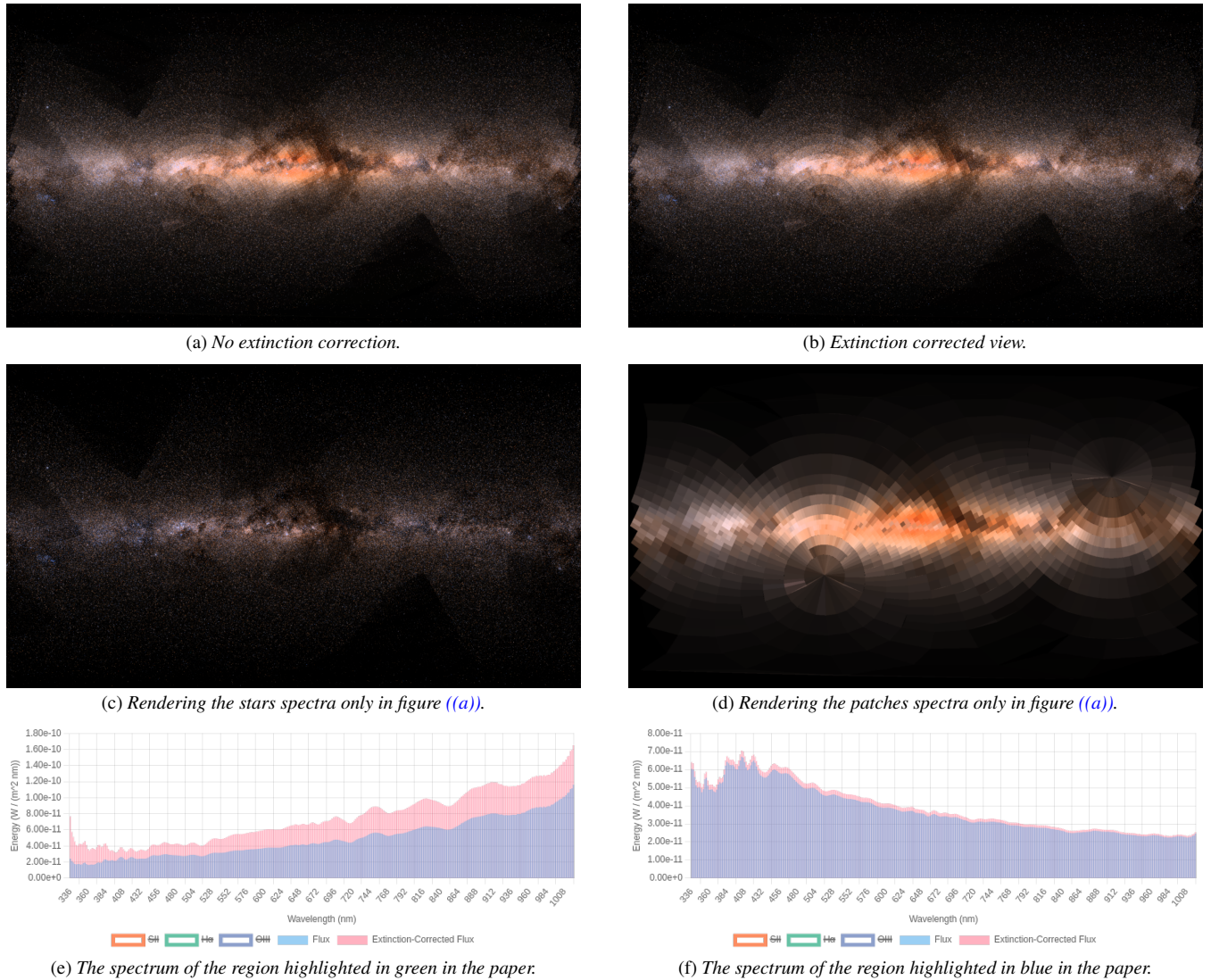


Figure 4: This is the extended version of Figure 10 in the paper, which shows the whole dataset in galactic coordinates, colored by convoluting with CIE sensitivity function. The full convergence time of the spectral buffer took 1.6 min, while the final renders are fully real-time. The star and patch spectral composition is demonstrated in figure (a): figure (c) renders the star spectra only, and the nodes at the graph cut are discarded. Figure (d) shows the opposite: only the nodes at the graph cut are rendered as patches in the sky. (a) shows the visualization using the raw spectra: gasses at the center of the galaxies are scattering light, causing a loss of intensity (interstellar extinction). (b) is rendered using the extinction-corrected spectra. Some regions are now brighter. (e) and (f) are the spectra of the region highlighted in green and blue in the paper respectively. The spectra are blue for the raw spectra and red after correction. (f) This is a spectrum of an area that is not obscured by interstellar gas, so the correction was minimal. In comparison, (e) is the gas-scattered spectra of an obscured region, so the correction amplified the intensities to compensate for the lost energy.

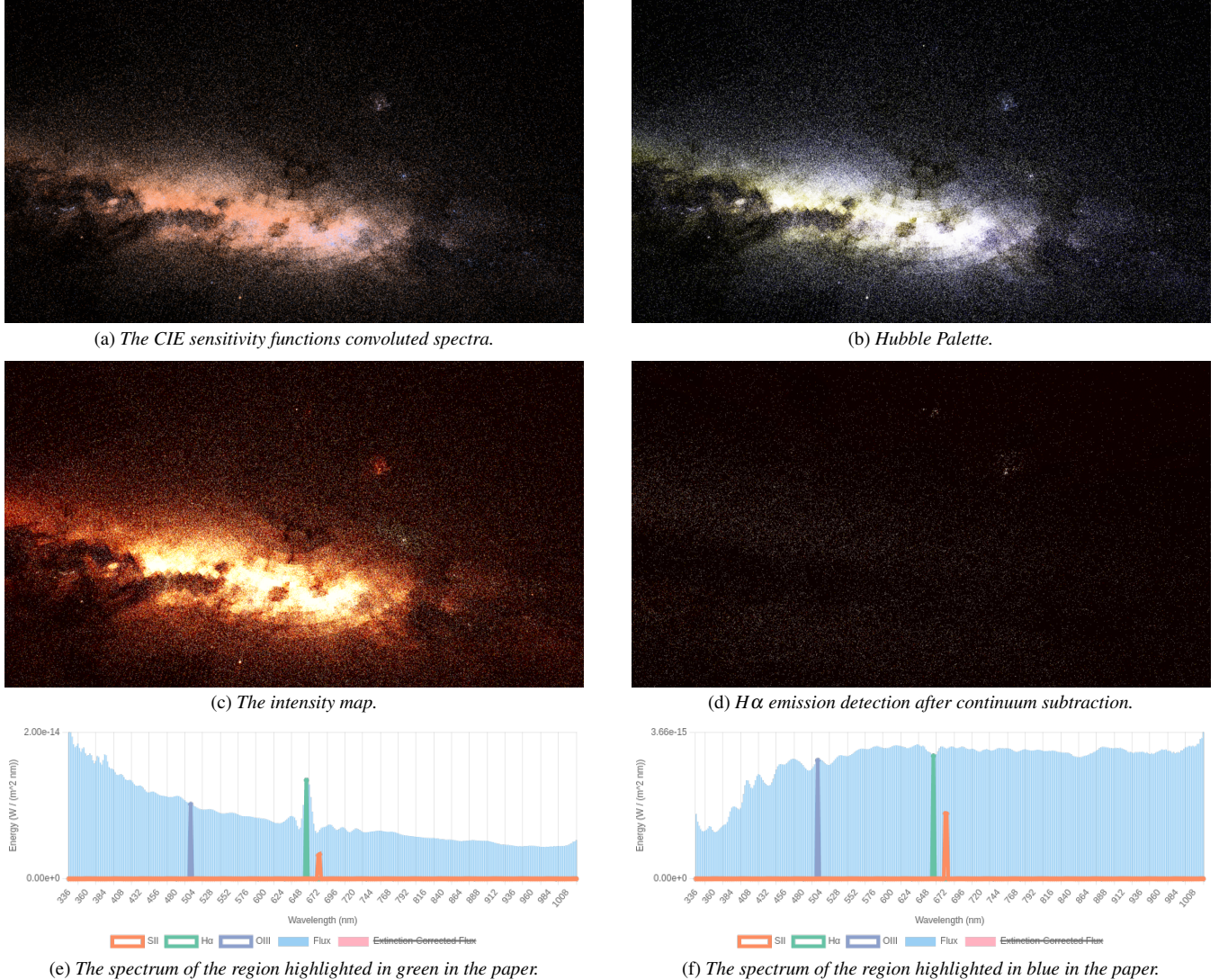


Figure 5: This is the extended version of Figure 11 in the paper, which shows the Magellanic Clouds and part of the Milky Way in spherical projection. The full convergence time of the spectral buffer took 1.9 min, while the final renders are fully real-time. The colors in (a) is the normalized convolution with CIE sensitivity functions and scaled by the intensity, while (c) is obtained based on the energy. (b) is an example of narrowband filtering and (d) is an example of emission line detection. (e) and (f) are the spectra of the region highlighted in green and blue in the paper, respectively. The spectrum is in blue, while the transmission functions modeled as a Gaussian centered around $SII = 673\text{nm}$, $H\alpha = 656\text{nm}$, and $OIII = 500.7\text{nm}$ are in orange, green, and purple, respectively. In (e), the spectrum has a hydrogen emission line, while (f) is the spectra of a region with a hydrogen absorption line. Consequently, The region highlighted in green in the paper was still bright after subtracting the continuum. On the other hand, the region highlighted in blue in the paper appears dark, as no hydrogen emission is detected there.